Tunable functionality and toxicity studies of titanium dioxide nanotube layers

E. Feschet-Chassot, V. Raspal, Y. Sibaud, Ok Awitor, Frédérique Bonnemoy, Jl Bonnet, Jacques Bohatier

Tunable Functionality and Toxicity Studies of Titanium Dioxide Nanotube Layers

E. Feschet-Chassot[a], V. Raspal[a], Y. Sibaud[a], O. K. Awitor[a,*], F. Bonnemoy[b], J.L.Bonnet[b,c], J. Bohatier[b,c]

[a] *Clermont Université, Université d'Auvergne, C-BIOSENSS, BP 10448, F-63000 Clermont Ferrand*
[b] *Clermont Université, Université Blaise Pascal, UMR CNRS 6023, LMGE, BP 10448, F-63000 Clermont Ferrand*
[c] *Clermont Université, Université d'Auvergne, Laboratoire de Biologie cellulaire, BP 10448, F-63000 Clermont Ferrand*

Abstract

In this **study**, we have developed **a simple** process to **fabricate** scalable titanium dioxide nanotube layers which show a tunable functionality. The titanium dioxide nanotube layers were prepared by electrochemical anodization of Ti foil in 0.4 wt% hydrofluoric acid solution. The nanotube layers structure and morphology were characterized using x-ray diffraction and scanning electron microscopy. **The surface topography and wettability were studied according to the anodization time. The sample synthesized displayed a higher contact angle while the current density reached a local minimum**. Beyond this point, the contact angles decreased with anodization time. Photo-degradation of acid orange 7 in aqueous solution was used as a probe to assess the photocatalytic activity of titanium dioxide nanotube layers under UV irradiation. We obtained better photocatalytic activity for the sample **fabricated** at higher current density. Finally we used the Ciliated Protozoan *T. pyriformis*, an alternative cell model used for in vitro toxicity studies, to predict the toxicity of titanium dioxide nanotube layers in a biological system. We did not observe any characteristic effect in the presence of the titanium dioxide nanotube layers on two physiological parameters related to this organism, non-specific esterases

*Corresponding author
Email address: koawitor@iut.u-clermont1.fr ()

activity and population growth rate.

Keywords:
Anodization, Titanium Dioxide Nanotubes, Contact Angle,
Photodegradation, Toxicity.

1. Introduction

Research into developing nanotubes with **interesting** properties by controlling the nanostructure topography has attracted great interest because of their variety of applications. In 2001, Gong and co-workers [1] reported the fabrication of vertically oriented highly ordered TiO_2 nanotube arrays up to approximately 500 nm length by anodization of titanium foil in an aqueous HF electrolyte. Since then, substantial efforts have been devoted to the self organisation and growth of TiO_2 [2, 3, 4]. Titanium dioxide nanotube layers are used as photo-catalysts in water and environmental purification, as well **as biological** and biomedical applications [5, 2, 6]. In particular, Titanium dioxide nanotubes are used as a **biomaterial** for implants, drug delivery platforms, tissue engineering and bacteria killing [7, 8, 9, 10, 11, 12, 13]. Another interesting propriety of TiO_2 is its tunable wettability effect [14, 15]. The ability to modify surface topography and to control wetting behavior is useful for biomedical applications. Surface roughness, contact angle, surface energy are the main factors in understanding the biology media and material interaction. In this work, we present recent results on TiO_2 nanotubes fabricated by anodization of Ti foil in 0.4 wt% hydrofluoric acid solution to produce a self-organized porous film structure versus the anodization time. Such TiO_2 nanotube surfaces are of interest in order to change the wettability properties of titanium oxide films. The nanotube layers were characterized using x-ray diffraction and scanning electron microscopy. We have investigated the surface wettability of as-anodized samples obtained at different anodization times. The as-grown sample synthesized while the current density **reached** a local minimum displayed higher contact angle. The surface of the oxide was covered at this point with a high density of fine pits. **We report on the photo-degradation of acid orange 7 (AO7) in aqueous solutions which was used as a probe to assess the photocatalytic activity of titanium dioxide nanotube layers under UV irradiation.** We obtained better photocatalytic activity for the sample **fabricated** at higher current density. Finally we **used** the Ciliated Protozoan *T. pyriformis* to predict the

toxicity of titanium dioxide nanotube layers towards biological systems.

2. Experimental Details

2.1. Sample preparation

To fabricate anodic TiO_2 nanotube layers, we used Ti foil (Goodfellow 99.6% purity) with a thickness of 0.1 mm. The Ti foils were degreased by successive sonication in trichloroethylene, acetone and methanol, followed by rinsing with deionized water, dried in the oven at 100°C and finally cooled in the desiccator. Anodization was carried out at room temperature (20°C) in 0.4 wt% HF aqueous solution with the anodizing voltage maintained at 20 V.

2.2. Surface characterization

The surface topography characterization was performed using a Zeiss Supra 55 VP scanning electron microscope (SEM) **with secondary emission and in lens detector. The accelerating voltage and the working distance are respectively 3kV and 5mm**. **The crystalline structure and phase of the** TiO_2 **nanotube layers were determined by X-ray diffraction (XRD) using a Scintag XRD X'TRA diffractometer with Cu**K_α **(λ = 1.54 Å) radiation. The Cu**K_β **radiation is filtered through a nickel filter. The diffraction pattern was achieved between 20 and 80° with a step angle of 0.05° and a scanning speed of 0.01° per second.**

2.3. Contact angles

Surface wettability **was** investigated using a drop shape analysis system (EasyDrop, Kruss, Hambourg, Germany). The contact angle of 3 μL sessile droplet of deionized water was measured on the surface under ambient conditions.

2.4. Photo-degradation

Photocatalytic experiments were conducted in 3 mL of AO7 solution (from Acros Organics) with a concentration of 5.0 10^{-5} mol/L, placed in a cylindrical Pyrex glass reactor. The surface area of the anodized samples was approximately 3.5 cm^2. The glass reactor was irradiated with polychromatic fluorescent UV lamps (Philips TDL 8 Watt (total optical power 1.3 Watt), 300 mm long, wavelength range 315-400 nm) in a configuration providing

about 0.9 mW/cm^2 at the sample surface. The photocatalytic decomposition of AO7 was monitored by the decrease in the solution's absorbance at a wavelength of 485 nm using a UV-Vis spectrometer (Perkin Elmer Lambda 35).

2.5. Toxicity assessment

The potential toxicity of TiO_2 nanotube surfaces was evaluated with *Tetrahymena pyriformis* using two tests previously validated : inhibition of an enzymatic activity and effect on population growth rate. For non-specific esterases activities quantification, a *T. pyriformis* culture in an exponential growth phase (in PPYS medium) was centrifuged at 300 rpm, and the supernatant was discarded. The *T. pyriformis* pellet was suspended in Volvic mineral water. After counting cells under a microscope, dilution was done to obtain about 4000 cells/mL. 1 mL of this dilution was incubated for 1h with the different Ti layers at 28 °C under UV or without UV irradation. After incubation, Ti layers samples were removed and 1 mL of **Fluorescein diacetate (FDA)** at 4.8 μM was added (2000 cells/mL in final). Each toxicity test included two controls : FDA in Volvic water to measure self degradation of this substrate and FDA with *Tetrahymena pyriformis* (untreated cells). After 30 min, the fluorescence was measured by a spectrofluorimeter (Kontron SFM 25, Kontron, Milan, Italy) with a 485 nm excitation filter and a 510 nm emission filter. Experiments were repeated three times for each sample. To test the inhibition of development of populations in an exponential growth phase, we prepared 8 erlenmeyer flasks (40 mL): 2 for control cultures and 6 for the samples to be tested (Ti foil, unannealed TiO_2 and TiO_2 annealed at 500 °C). The samples were deposited at the bottom of the erlenmeyer flasks and 3 mL were **removed** at 0h, 3h, 6h and 9h to measure the optical density (OD) at 535 nm.

3. Results and discussion

3.1. TiO_2 Nanotube growth process and Layer Characteristics

The anodization growth was governed by a competition between anodic oxide formation and chemical dissolution [16] of the oxide as soluble fluoride complexes according respectively to reactions (1) and (2) :

$$Ti \ + \ 2\ H_2O \ \rightarrow \ TiO_2 \ + \ 4\ H^+ \ + \ 4\ e^- \qquad (1)$$

$$TiO_2 \ + \ 4\ H^+ \ + \ 6F^- \ \rightarrow \ [TiF_6]^{2-} \ + \ 2\ H_2O \qquad (2)$$

Figure 1 shows a characteristic density current time curve for Ti anodization in our operating conditions and figure 2 shows SEM images of the TiO_2 grown at different stages of growth corresponding to the points a, b, c and d. We can notice that after an initial exponential decay of the current density to a local minimum around 10 mA.cm^{-2} about 70 s. The structure of the film at this point led to the formation of randomly generated pits on the oxide which were shown in figure 2a. The pits were approximately 30 nm in diameter.

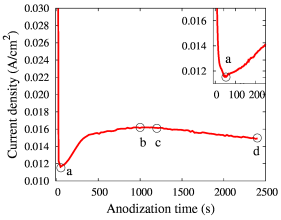

Figure 1: Typical density current time curve for Ti foil anodization. Anodization was carried out at room temperature (20°C) in a 0.4 wt% HF aqueous solution with the anodizing voltage maintained at 20V. Inset in upper right hand conner shows a blow up of the time behavior from 0 to 250 s.

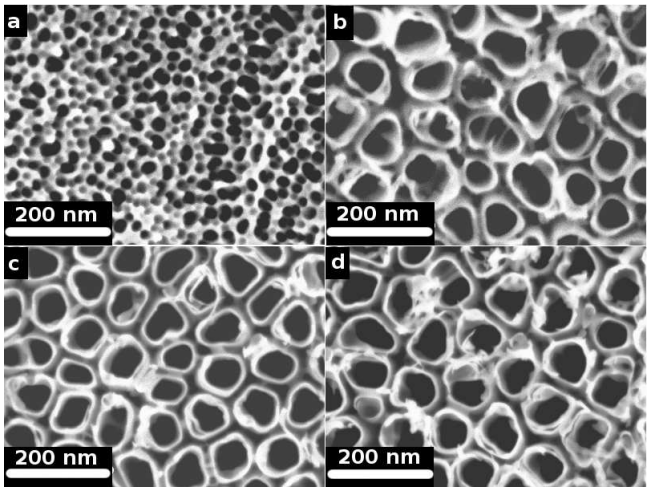

Figure 2: SEM top-view images of samples taken while density current was at local minimum (a), local maximum (b) and at the anodization time of 20 min and 40 min respectively (c, d).

After the current density increased to a local maximum of 12,7 mA.cm^{-2}

in 1000 s, we **observed** ordered nanotube arrays with approximately 85 nm in diameter as evidenced by figure 2b. After 20 min and 40 min of growth, we observed in figure 2c and 2d ordered nanotube arrays with approximately 100 nm and 105 nm in diameter respectively. We summarize in figure 3, the evolution of the diameter of the pores. Between 70 and 1000 s, we **observed** a linear evolution of the diameter versus time with a high slope. Similarly, the trend is weak between 1000 and 2400 s. At 2400 s, we reach the maximum diameter. This shows that the dissolution rate of oxide is predominant over the oxide growth velocity. So in a steady state, the pore diameters do not depend on the anodization time despite enlargement of the pore diameters due to the dissolution of the mouth of the nanotubes as reported elsewhere [17].

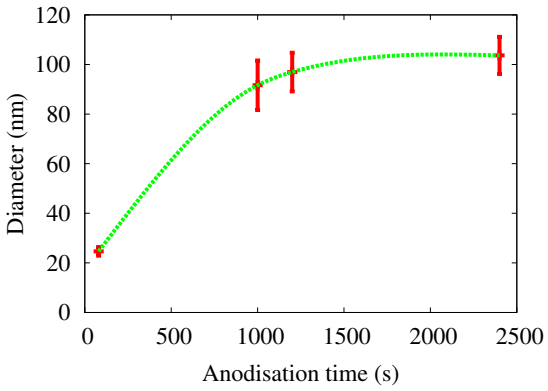

Figure 3: The evolution of the diameter of the pores of **samples** (a), (b), (c) and (d).

We summarize in figure 4 the X-ray diffraction patterns of Ti foil and TiO_2 nanotube layers anodized for 40 min before and after annealing at 500°C in oxygen for 2 h according to the paper published elsewhere [2]. The unannealed TiO_2 nanotube layer exhibits only the peaks from titanium metal foil under the nanotube layer, while the annealed sample exhibits the main lattice phases of anatase and rutile (figure 4).

3.2. Contact angles

The influence of TiO_2 nanotubes on Ti on bone cell-materials interaction has been reported [18]. In this study, we have evaluated the contact angle behavior on TiO_2 nanotube layers which have pronounced topological features and increased surface areas. Contact angles were measured for

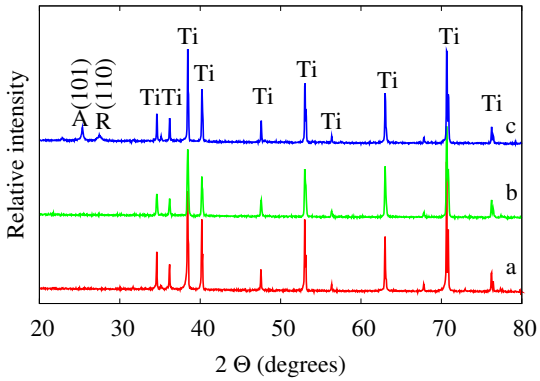

Figure 4: X-ray diffraction patterns of Ti foil (a), as grown during 40 min (b) and annealed TiO_2 nanotube layers at 500°C in oxygen for 2 h (c). Lattice planes indicate anatase (A), rutile (R) and titanium (Ti).

each as-anodized sample. Each sample was dried in the oven for 30 min and cooled 15 min in the desiccator before measurements. We observe in figure 5, optical images of water droplets on as-grown TiO_2 nanotube layers. Results indicated a higher contact angle for the sample covered with pits obtained at local minimum density current (70 s). Beyond this particular point, the contact angles value decreases with anodization time. So we have performed a scalable surface functionality without any chemical treatment.

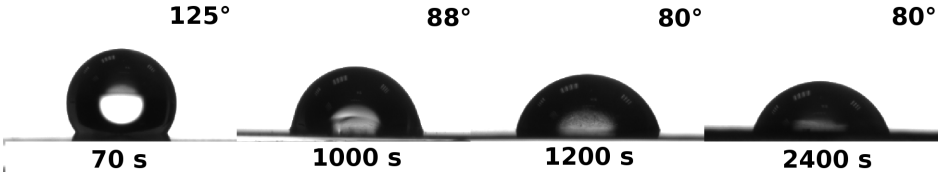

Figure 5: Optical images of water droplets on as-grown TiO_2 nanotube layers. Surface at local minimum density current (70 s); surface at local maximum density current (1000 s); surface after 20 min of growth (1200 s) and surface after 40 min of growth (2400 s).

3.3. Photo-catalytic activity measurement

The photo-degradation of AO7 in the presence of TiO_2 nanotubes under different conditions is summarized in figure 6. This shows the AO7 concentration versus time as determined by the solution's absorbance at 485 nm. The initial concentration of the AO7 was 5.0 10^{-5} mol/L. C(0) is the initial

concentration of AO7 while C(t) is the concentration after time, t, of constant UV irradiation in 315-450 nm wavelength range. The variation of the concentration of AO7 in the presence of the TiO_2 layer without irradiation after 5 h is less than 1%. Thus the effect of adsorption of the dye on the TiO_2 surface is negligible. Curve 6(e) shows the variation in the concentration of AO7 in the presence of unannealed TiO_2 nanotubes under UV irradiation. This result indicates that AO7 is not substantially degraded in the presence of amorphous TiO_2 nanotube layers. Curves 6(a), 6(b), 6(c) and 6(d) corresponding to the TiO_2 nanotube layers grown during 70 s, 1000 s, 1200 s, 2400 s respectively and annealed at 500°C illustrate photo-degradation of AO7. These results show the decay of organic molecules with UV irradiation in the presence of the annealed nanotubes. We observed the strongest photocatalytic activity for the sample grown during 1200 s. We **cannot** draw any correlation between surface wettability and photocatalytic activity.

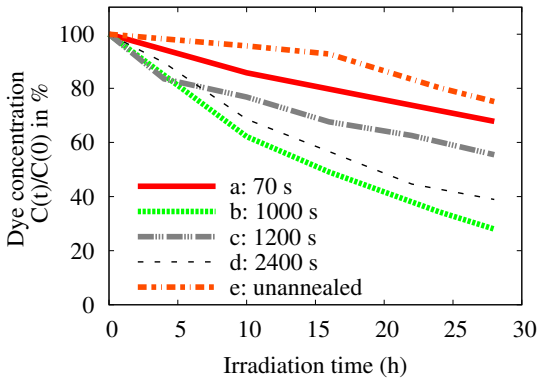

Figure 6: Photo-degradation of acid orange 7 (AO7) dye under UV-lamp irradiation at wavelengths of 315-400 nm in the presence of a TiO_2 nanotube layer, as measured by the absorbance of the irradiated dye at 485 nm. C(0) is the initial concentration of AO7 ($5\ 10^{-5}$ M) and C(t) is the concentration after time, t, of irradiation. **(e)** unannealed TiO_2 nanotube layer; (a), (b), (c), (d) TiO_2 nanotube layers grown during 70 s, 1000 s, 1200 s, 2400 s respectively and annealed at 500°C.

The effect of irradiation of the sample grown for 1000 s with polychromatic light (315-400 nm) on the UV-Vis spectrum is **shown in figure** 7. Absorbance for increasing irradiation time decreases from the upper curve toward the lower curve.

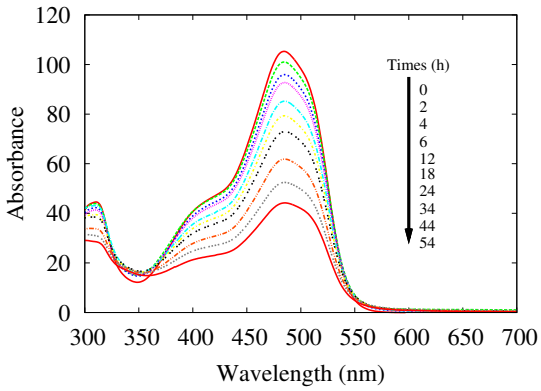

Figure 7: Effect of irradiation with polychromatic light (315-400 nm) of AO7 in the presence of TiO_2 nanotube layers grown during 1000 s and annealed at 500°C on the UV-Vis spectrum in the 300-700 nm range.

3.4. Toxicity tests

The cellular toxicity of TiO_2 based nanofilaments [19], nanoparticles [20] was studied. The authors concluded that these nanofilaments and nanoparticles are cytotoxic. However, in other studies, no toxic effects were observed with TiO_2 nanoparticles [21, 22]. Similarly the effects of radical reactivity generated by TiO_2 on cells under UV irradiation **is** still controversial [23, 24]. **As far as we know**, no study has been conducted on the toxicity of TiO_2 nanotube layers. In this work two different tests of toxicity have been made with the Ciliated protozoan *T. pyriformis* as described in detail elsewhere [25]. This organism is an alternative eukaryotic cell model including the established fibroblastic cell lines used **in vitro** toxicity studies. All the tests were carried out with titanium foil, amorphous and crystalline TiO_2 nanotube layers. The cristalline samples showed photocatalytic activities. We studied their influence under UV radiation on the toxicity tests. The test of inhibition of non-specific intracellular esterase activity was based on the hydrolysis of fluorescein diacetate (FDA) by *T. pyriformis* and quantification of fluorescein released **for** 30 min. Esterases are ubiquitous enzymes present in all living organisms and are considered as good biomarkers of cellular activities. The aim of this test was to determine the evolution of the percentage of the *T. pyriformis* activity over the control in the presence of Ti foils, amorphous and crystalline TiO_2 nanotube layers without UV irradiation **without UV)** and with constant UV irradiation (**With UV)** at a wavelength of 315-400 nm. We can observe an effect of titanium foil but

no significant effect of the amorphous and crystalline TiO_2 nanotube layers. The UV light radiation did not disturb the results (Figure 8) **despite** the photocatalytic activities of cristalline samples. Furthermore, *T. pyriformis* population growth rate test allows us to include different physiological disturbances which could have been caused by the three types of layers. Growth was followed photometrically with a measure of optical density (λ = 535 nm) every 3 hours. Reduction in growth compared to a control culture is indicative of toxicity.

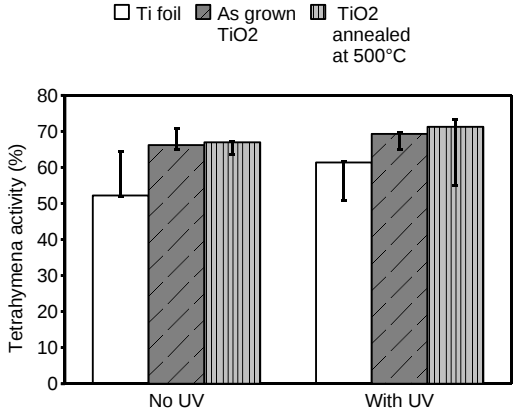

Figure 8: *T. pyriformis* activity over the control in the presence of Ti foil, amorphous and crystalline TiO_2 nanotube layers without UV irradiation (No UV) and with constant UV light (With UV) at wavelength range 315-400 nm.

The purpose of this test was to determine a 50% inhibition of growth rate in treated cultures (increase in 50% of the generation time compared to a control culture). We did not observe any characteristic effect related to the inhibition of protozoa growth for Ti foils, amorphous and crystalline TiO_2 nanotube layers (Figure 9). We can conclude through these two tests that the TiO_2 nanotube layers are not toxic.

4. Conclusions

We have demonstrated the fabrication of controllable as-grown surfaces of titanium dioxide nanotube layers. The contact angles measurements show clearly the correlation between surface topography and surface wettability. We have shown the ability of the titanium dioxide nanotube layers to degrade

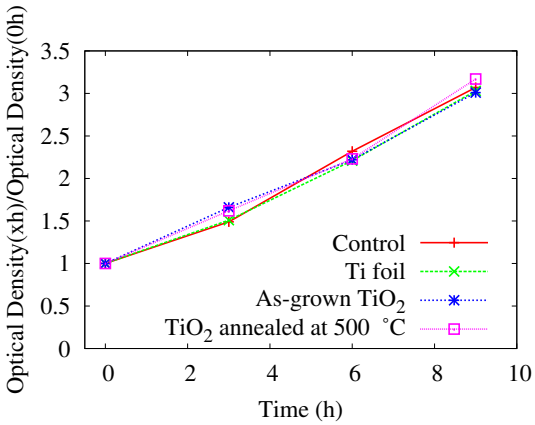

Figure 9: Growing populations of *T. pyriformis* in the presence of titanium foil, amorphous and crystalline titanium dioxide nanotube layers.

AO7. Such surfaces **do not** show any characteristic *in vitro* toxicity effect in a biological system. In conclusion, we have developed **a simple process** to **fabricate** active surfaces of titanium dioxide with scalable nanotube layers and tunable functionalities.

References

[1] D. Gong, C. Grimes, O. Varghese, W. Hu, R. Singh, Z. Chen, W. Hu, R. Singh, Z. Chen, J. Mater. Res. 16 (2001) 3331.

[2] J. M. Macak, M. Zlamal, J. Krysa, P. Schmuki, Small 3 (2007) 300.

[3] O. K. Varghese, D. Gong, M. Paulose, C. A. Grimes, E. C. Dickey, J. Mater. Res. 18 (2003) 156.

[4] V. Zwilling, M. Aucouturier, E. Darque-Ceretti, Electrochim. Acta 456 (1999) 921.

[5] K. Awitor, S. Rafqah, G. Géranton, Y. Sibaud, P. Larson, R. Bokalawela, J. Jernigen, M. Johnson, J. Photochem. Photobiol., A 199 (2008) 250.

[6] K. Sasaki, K. Asanuma, K. Johkura, T. Kasuga, Y. Okouchi, N. Ogiwara, S. Kubota, R. Teng, L. Cui, X. Zhao., Ann. Anat. 188 (2006) 137.

[7] K. Vasilev, Z. Poh, K. Kant, J. Chan, A. Michelmore, D. Losic, Biomaterials 31 (2010) 532.

[8] S. D. Puckett, E. Taylor, T. Raimondo, T. J. Webster, Biomaterials 31 (2010) 706.

[9] S. C. Roy, M. Paulose, , C. A. Grimes, Biomaterials 28 (2007) 4667.

[10] G. E. Aninwene, C. Yao, T. J. Webster, Int. J. Nanomed. 3 (2008) 257.

[11] I. Romana, C. Fratila, E. Vasile, A. Petre, M.-L. Soare, Mater. Sci. Eng., B 165 (2009) 207.

[12] K. C. Popat, L. Leoni, C. A. Grimes, T. A. Desai, Biomaterials 28 (2007) 3188.

[13] C. Yao, T. J. Webster, J. Biomed. Mater. Res. B Appl. Biomater. 91B (2009) 587.

[14] Y.-Y. Song, F. Schmidt-Stein, S. Bauer, P. Schmuki, J. Am. Chem. Soc. 131 (2009) 4230.

[15] E. Balaur, J. Macak, H. Tsuchiya, P. Schmuki, J. Mater. Chem. 15 (2005) 4488.

[16] J. Macak, H. Tsuchiya, A. Ghicov, K. Yasuda, R. Hahn, S. Bauer, P. Schmuki, Curr. Opin. Solid State Mater. Sci. 11 (2007) 3.

[17] Z. Su, W. Zhou, J. Mater. Chem. 19 (2009) 2301.

[18] K. Das, S. Bose, A. Bandyopadhyay, J. Biomed. Mater. Res. 90A (2009) 225.

[19] A. Magrez, L. Horváth, R. Smajda, V. Salicio, N. Pasquier, L. Forró, B. Schwaller, ACS Nano 3 (2009) 2274.

[20] W. F. Vevers, A. N. Jha, Ecotoxicology 17 (2008) 410.

[21] C. A. J. Dick, D. M. Brown, K. Donaldson, V. Stone, Inhalation Toxicol. 15 (2003) 39.

[22] T. Xia, M. Kovochich, Nano Lett. 6 (2006) 1794.

[23] C. M. Sayes, R. Wahi, P. A. Kurian, Y. Liu, J. L. West, K. D. Ausman, D. B. Warheit, , V. L. Colvin, Toxicol. Sci. 92 (2006) 174.

[24] I. Fenoglio, G. Greco, S. Livraghi, B. Fubini, Chem. Eur. J. 15 (2009) 4614.

[25] P. Bogaerts, J. Bohatier, F. Bonnemoy, Ecotoxicol. Environ. Saf. 49 (2001) 292.